Taylor & Francis
Taylor & Francis Group

Journal of Asian Architecture and Building Engineering

ISSN: 1346-7581 (Print) 1347-2852 (Online) Journal homepage: https://www.tandfonline.com/loi/tabe20

Hydration Heat and Autogenous Shrinkage of High-Strength Mass Concrete

Gyuyong Kim, Euibae Lee & Kyungmo Koo

To cite this article: Gyuyong Kim, Euibae Lee & Kyungmo Koo (2009) Hydration Heat and Autogenous Shrinkage of High-Strength Mass Concrete, Journal of Asian Architecture and Building Engineering, 8:2, 509-516, DOI: 10.3130/jaabe.8.509

To link to this article: https://doi.org/10.3130/jaabe.8.509

Hydration Heat and Autogenous Shrinkage of High-Strength Mass Concrete

Gyuyong Kim[1], Euibae Lee*[2] and Kyungmo Koo[2]

[1] Professor, Department of Architecture Engineering, Chungnam National University, Korea
[2] Graduate Student, Department of Architecture Engineering, Chungnam National University, Korea

Abstract

In this study, to evaluate autogenous shrinkage of high-strength mass concrete with specimen size and hydration delay effects, the thermal deformation was calculated using thermal expansion coefficient (TEC) corrected by the maturity method, and was subtracted from measured total deformation. And the properties and relations of hydration heat and autogenous shrinkage at early ages were numerically analyzed. In test and analysis results, hydration temperature is affected by specimen conditions such as size and admixture, and change of hydration temperature could affect autogenous shrinkage; the higher hydration temperature and the greater autogenous shrinkage. There is a close relationship between hydration temperature and autogenous shrinkage at early ages, especially between HHV (hydration heating velocity) and ASV (autogenous shrinking velocity); the higher HHV, the higher ASV and the greater ultimate autogenous shrinkage. The points where hydration temperature and autogenous shrinkage start to increase rapidly are due to the consumption of gypsum in the cement hydration process, and are strongly related to the setting time.

Keywords: high-strength mass concrete; hydration heat; autogenous shrinkage

1. Introduction

High-strength concretes are characterized by high binder content coupled with low water/binder ratio. These features contribute to the high hydration temperature and enormous autogenous shrinkage (Sioulas *et al*. (2000) and Lura *et al*. (2003)). Autogenous shrinkage should be limited because it may induce micro or macro cracking and impair the concrete quality (Paillere *et al.*, 1989).

Recently, the construction of ultra high-rise buildings is increasing due to the social demands. In such buildings, the high-strength concrete is being applied and the size of members increased. In massive members, the inner temperature rise more and more because of high hydration heat and the isolation effect of concrete. Therefore, it is necessary to consider the inner high temperature history in evaluating the autogenous shrinkage of massive members made with high-strength concrete.

Bjøntegaard *et al*. (1997) and Horita *et al*. (2001) reported that the magnitude and rate of development of autogenous shrinkage depends strongly on the entire temperature history of the concrete following mixing. Also autogenous shrinkage increases in high temperature even in the same mortar or concrete in studies by Loukili *et al*. (2000) and Shima *et al*. (2006). And most autogenous shrinkage of high strength concrete with low W/C or W/B was formed in a few days from casting (Shima *et al.*, 2006). In consideration of these studies, it could be found that the relationship between hydration temperature and autogenous shrinkage at early ages is important to understanding the whole autogenous shrinkage of high-strength mass concrete.

Kim *et al*. (2008) and Lee *et al*. (2008) suggested an analysis method regarding the histories of hydration heat and autogenous shrinkage at early ages. On the basis of this, in this study, the early age properties and relations of hydration heat and autogenous shrinkage of high-strength mass concrete with the conditions of specimen size and hydration retardation were numerically investigated. Also the history shapes of hydration temperature and autogenous shrinkage were investigated from the viewpoint of the chemical reaction of cement.

2. Experimental Plan and Methods

2.1 Experimental plan

Table 1. shows the conditions of the specimens for the experiment. There are three different specimen sizes to vary hydration temperature histories; 100×100 ×400mm, 150×150×600mm and 300×300×300mm. The 300×300×300mm specimen was made in a semi-

*Contact Author: Euibae Lee, Graduate Student, Department of Architecture Engineering, Chungnam National University
79 Daehangno, Yuseong-gu, Daejeon, 305-764 Korea
Tel: +82-42-821-7731 Fax: +82-42-823-9467
E-mail: mir2468@cnu.ac.kr
(Received April 7, 2009 ; accepted August 6, 2009)

Table 1. Conditions of Specimen

	Conditions of specimen			
Symbol	100^2×400	150^2×600	300^2×300	300^2×300-R
Size	100×100 ×400	150×150 ×600	300×300 ×300	300×300 ×300
Curing	In the air (20°C)	In the air (20°C)	Semi -adiabatic	Semi -adiabatic
Addition of retarder	-	-	-	0.3%
Type	Concrete	Concrete Mortar Paste	Concrete	Concrete

Table 2. Mixture Proportions of Concrete

W/C (%)	Slump-flow (mm)	S/a	Unit weight (kg/m^3)				HRWR (C×%)
			W	C	G	S	
20	650±50	0.47	160	800	781	664	1.0

Table 3. Materials

Materials	Physical and chemical properties
Cement	▪ Ordinary portland cement ▪ Density : 3.15g/cm^3 ▪ Fineness : 3,770cm^2/g
Fine aggregate	▪ Desalting sand ▪ Max size : 5mm ▪ Density : 2.54g/cm^3 ▪ F.M. : 3.05 ▪ Absorption ratio : 1.01
Coarse aggregate	▪ Crushed aggregate ▪ Max size : 20mm ▪ Density : 2.65g/cm^3 ▪ F.M. : 6.02 ▪ Absorption ratio : 1.39
Retarder	▪ Gluconic acid type
High range water reducer	▪ Polycarboxylic acid type

adiabatic condition considering the insulation effect of the massive member. Also, to examine the effect of hydration delay, an additional specimen with a size of 300×300×300mm, and added retarder of 0.3%, was made. To investigate the relation between setting time and histories of hydration temperature and autogenous shrinkage, a mortar specimen with a size of 150×150×600mm was made. And, to confirm the change of cement ingredient and hydrates, a cement paste specimen with a size of 150×150×600mm was made. The samples for the XRD analysis were gathered at the initial setting time, final setting time and after 1 day following casting.

2.2 Materials and mix proportion

The mixture proportion of concrete is shown in Table 2. Water/cement (W/C) ratio was 20% and the unit weight of cement was 800kg/m^3. Details concerning the kinds and properties of materials are shown in Table 3.

2.3 Specimen and test methods

The schematics of the specimen and test method are shown in Fig.1. The 300×300×300mm specimen was cast in a mold made with expandable polystyrene board with a thickness of 100mm. To reduce the friction between concrete and the mold, a double layer of PVC

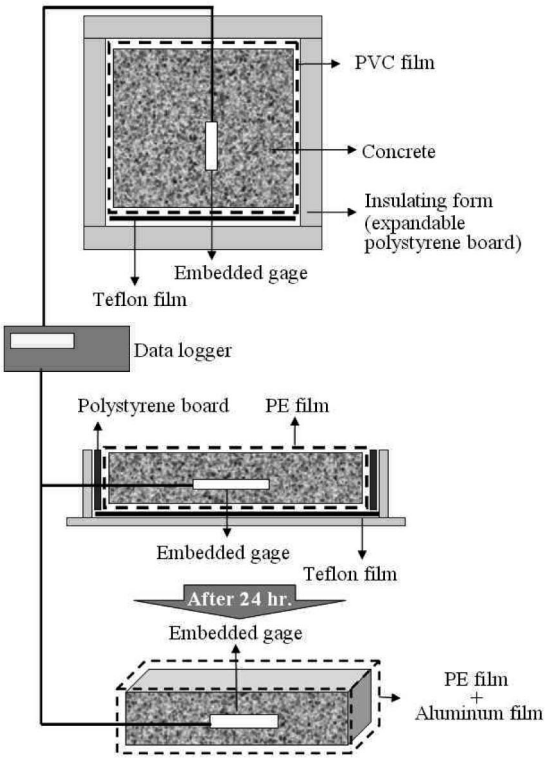

Fig.1. Schematic of Test Method for Hydration Temperature and Deformation of Concrete

film and teflon film were used. The temperature and deformation of the 300×300×300mm specimen were measured continuously without removal of the mold. The molds of specimens with 100×100×400mm and 150×150×600mm were removed after 24 hours from the casting. The specimens were wrapped with PE film and aluminum adhesive tape to prevent the moving of moisture. The inner temperature and deformation of the specimen were measured by thermocouple and embedded gage every ten minutes following casting.

Autogenous shrinkage of the 100×100×400mm specimen can be investigated excluding thermal effect on the assumption of the quasi-isothermal condition (Aïtcin, 1999). But, because the temperature in the 300×300×300mm semi-adiabatic specimen greatly increased, to evaluate autogenous shrinkage more exactly, measured deformation should be corrected for the thermal deformation. So, in this study, total deformation was corrected by Eq. (1).

$$\varepsilon_{auto} = \varepsilon_{total} - \varepsilon_{thermal} \quad (1)$$

Where, ε_{auto}: autogenous shrinkage ($\times 10^{-6}$)
ε_{total}: measured total deformation ($\times 10^{-6}$)
$\varepsilon_{thermal}$: thermal deformation ($\times 10^{-6}$)

Thermal deformation can be calculated by Eq. (2).

$$\varepsilon_{thermal} = \gamma \times \Delta t \quad (2)$$

Where, γ: linear thermal expansion coefficient (TEC) of specimen ($\times 10^{-6}$/°C)
Δt: temperature change (°C).

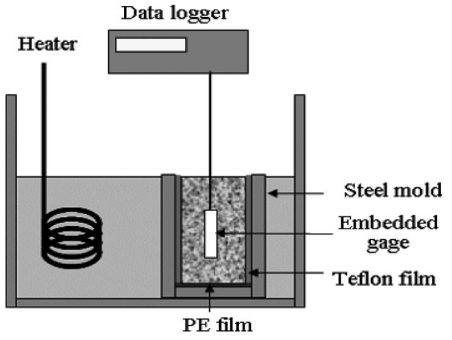

Fig.2. Schematic of Test Method for Thermal Expansion Coefficient of Concrete

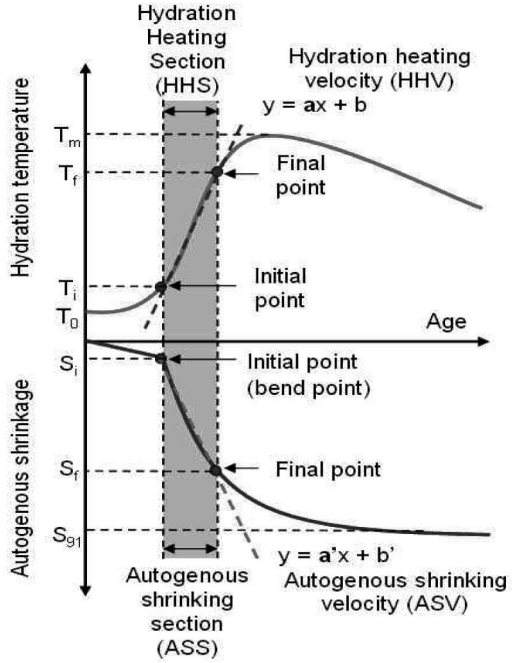

Fig.3. Analysis Method for Histories of Hydration Temperature and Autogenous Shrinkage

The TEC of concrete (γ) varies according to its mixture proportions and materials, and it should be carefully measured. Moreover, it is difficult to evaluate the TEC of concrete in the early ages since its phase and microstructure change with time. If rise in temperature is sufficiently fast, the measured deformation will be only of thermal origin (Loukili *et al*., 2000). In this study, *Φ*100×200mm cylinder specimen embedded thermocouple and strain gage was cast and immersed in a water bath as shown in Fig.2. The temperature of the bath was initially about 20°C and increased about 15°C during 10 minutes. Then the temperature change (Δt) and amount of expansion (Δε) were measured, and finally TEC (Δε/Δt) of concrete was calculated with age.

2.4 Analysis methods

To analyze numerically early age properties of hydration heat and autogenous shrinkage, Kim *et al*. (2008) and Lee *et al*. (2008) centered on two sections where hydration temperature and autogenous shrinkage rapidly increase; hydration heating section (HHS) and autogenous shrinking section (ASS). And statistical methods to set HHS and ASS were suggested. HHS and ASS were determined by regression analysis with a determination coefficient of over 0.95 from the datum points. The datum point of HHS was the final point; the point of 80% of maximum temperature rise, and it was determined by analyzing the histories drawn by the adiabatic temperature equation. The datum point of ASS was the bend point (turning point (Horita *et al*. (2001)), mentioned as bend point in this study). Table 4. shows a summary of the factors used in the analysis.

On the basis of this analysis method, in this study, the early age properties and the relations of hydration heat and autogenous shrinkage of high strength mass concrete were investigated.

Table 4. Factors for HHS and ASS Analysis

	Sections and Factors	Definition and calculation methods
HHS	Initial point	▪ The point having a determination coefficient of 0.95 by regression with the final point
	Final point	▪ The point of 80% of the maximum temperature rise ▪ Final point = $T_0+(T_m-T_0)\times0.8$
	Temperature rise	▪ Amount of temperature increased during HHS ▪ Rise = $T_f - T_i$
	Temperature rise ratio	▪ The proportion of temperature rise to maximum temperature rise ▪ Ratio=$(T_f - T_i)/(T_m-T_0)\times100$
	Hydration heating velocity (HHV)	▪ The linear slope of HHS ▪ The regression coefficient (a)
ASS	Initial point	▪ Initial point =bend point
	Final point	▪ The point having a determination coefficient of 0.95 by regression with the initial point
	Shrinkage rise	▪ The amount of autogenous shrinkage increased during ASS
	Shrinkage rise ratio	▪ The proportion of autogenous shrinkage rise to autogenous shrinkage at 91 days
	Autogenous shrinking velocity (ASV)	▪ The linear slope of ASS ▪ The regression coefficient (a')

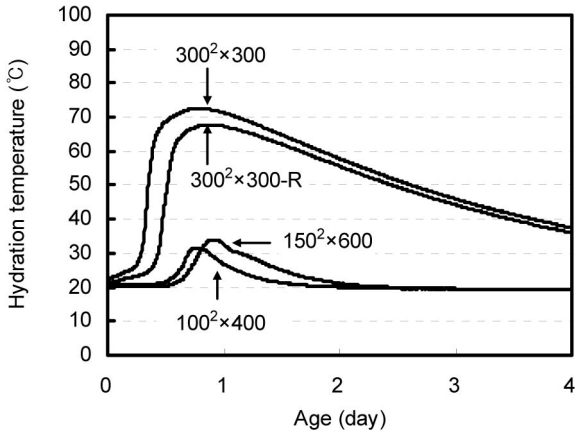

Fig.4. Histories of Hydration Temperature

Table 5. Analysis Results of HHS

Symbol	Hydration heating section (HHS)							Maximum temperature
	Initial point		Final point		Regression equation	HHV (°C/hr.)	Length of time (hr.)	
	Time (hr.)	Temp. (°C)	Time (hr.)	Temp. (°C)				
100^2×400	11.5	21.3	16.7	29.7	Y = 1.91+1.59X	1.59	5.2	10.7
150^2×600	13.0	20.7	19.5	31.1	Y = -2.07+1.63X	1.63	6.5	13.7
300^2×300	5.5	25.8	9.7	62.5	Y = -34.7+9.90X	9.90	4.17	51.0
300^2×300-R	8.7	25.0	13.3	58.8	Y = -50.2+8.01X	8.01	4.67	47.1

Table 6. Measurement of the Temperature Change and the Expansion in Φ100×200mm Cylinder Specimen for TEC Test

No addition of retarder	Measuring age (hr.)	3	5	7	11	13	14.5	23.5	-	-	-
	Temperature change (Δt, °C)	7.4	5.9	4.6	3.9	5.3	6	5.3	-	-	-
	Expansion (Δε, $\times10^{-6}$)	452	34.5	261	84	117	100	50	-	-	-
Addition of retarder 0.3%	Measuring age (hr.)	1	3	5	8	9	11	12.5	20.5	24.5	30
	Temperature change (Δt, °C)	7.1	5.9	4.5	4.8	3.8	5.4	5.9	5.4	6.0	5.4
	Expansion (Δε, $\times10^{-6}$)	462	363	289	282	164	216	205	75	65	55

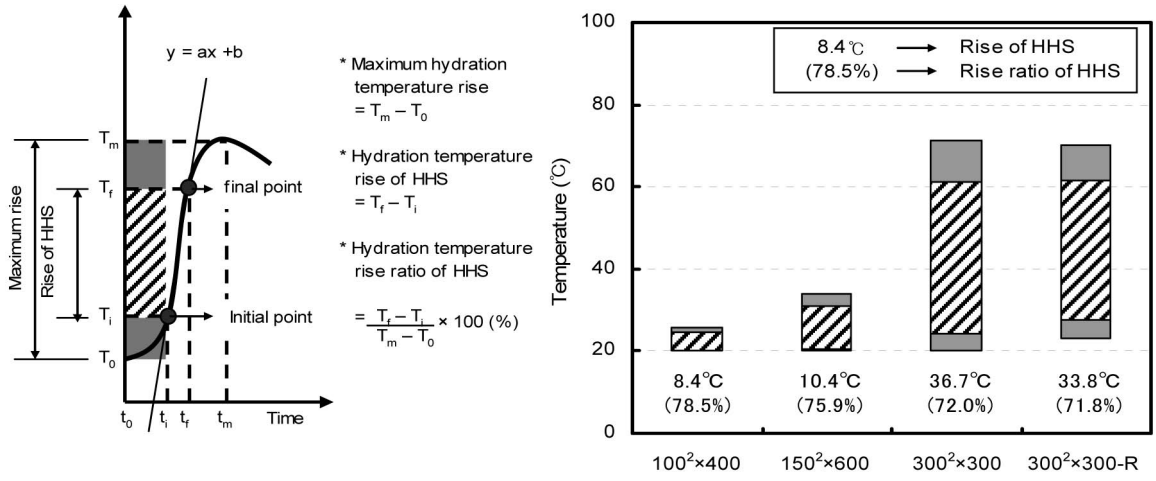

Fig.5. Hydration Temperature Rise of HHS and Rise Ratio to Maximum Temperature Rise

3. Results and Discussion

3.1 Analysis of hydration temperature

Fig.4. shows the histories of hydration temperature. The maximum temperatures of 100^2×400 and 150^2×600 are 32°C and 34°C. The maximum temperature of 300^2×300 increased by about 2.3times (73°C) compared with that of 100^2×400. In the case of 300^2×300-R, the maximum temperature is 67.7°C, a decrease of about 7% compared with that of 300^2×300.

Table 5. shows the analysis results of HHS and Fig.5. shows the hydration temperature rise and rise ratio to maximum temperature rise in HHS. Although there are differences of hydration temperature rise according to the specimen size and retarder, hydration temperature rise ratios of HHS are about 70-80%. HHVs of 100^2×400 and 150^2×600 are similar; 1.59°C/hr. and 1.63°C/hr. HHV of 300^2×300 increase by about 6 times (9.90°C/hr.) compared with that of 100^2×400. HHV of 300^2×300-R is calculated to 8.01°C/hr.. This shows that the HHV increases as the inner temperature (maximum temperature) increases.

3.2 TEC measurement and correction by maturity

At first, the temperature change and amount of expansion were measured through the TEC test. The measuring results are shown in Table 6, and TEC are calculated from them. Based on the measured TECs with age, TEC history could be calculated by regression. However, in the case of the 300×300×300mm semi-adiabatic specimen, TEC may change more quickly than that of the Φ100×200mm cylinder specimen due to the high inner temperature (Teramoto and Maruyama, 2008). At this time, the maturity method is very useful. The concept of maturity makes it possible to estimate the degree of advancement of the hydration reactions corresponding to the concrete hardening (Waller *et al*. (2004) and Turcry *et al*. (2002)) Fig.6. shows maturity results with the base temperature -10°C. In the case of Φ100×200, 100^2×400 and 150^2×600 specimen, little maturity differences between them are shown. But, in the case of 300^2×300 and 300^2×300-R, a wide difference can be observed and the rapid change of the concrete phase can be expected. Then the age factors were calculated and the TECs were corrected by them.

Fig.7. shows TEC histories corrected by maturity. TECs of Φ100×200, 100^2×400 and 150^2×600 are the

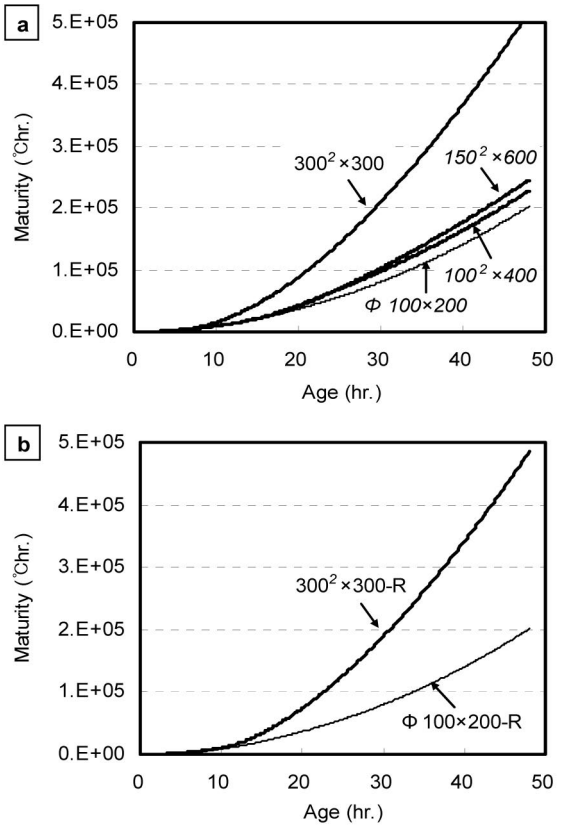

Fig.6. Maturity Results of the Various Specimens; (a) Specimen made without Retarder and (b) Specimen made with Retarder

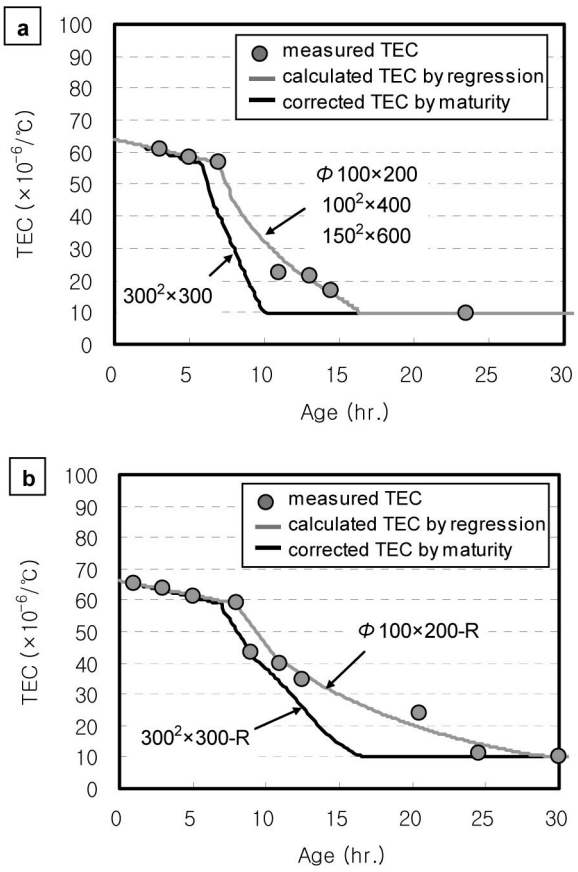

Fig.7. TEC Histories Corrected by Maturity; (a) Specimen made without Retarder and (b) Specimen made with Retarder

same regardless of maturity correction. The high TEC values observed at the early ages correspond to the time when the water phase dominates (Loukili *et al.* (2000) and Yang *et al*. (2005)). TEC decreases slowly and, after about 7 hours from casting, it decreases rapidly. Finally it converges to 9.5×10^{-6}/°C after about 16 hours from casting. The TEC of $300^2\times300$ decreases rapidly after about 6 hours from casting and converges after about 10 hours from casting. TEC of $300^2\times300$-R converges to 10.2×10^{-6}/°C after about 17 hours from casting.

3.3 Separation and analysis of autogenous shrinkage

To separate autogenous shrinkage from measured total deformation, it is necessary to calculate thermal deformation using the TEC and hydration temperature history. Thermal deformation is calculated by Eq. (3) proposed by Loukili *et al*. (2000).

$$\varepsilon_{thermal}(n)=\varepsilon_{thermal}(n-1)+\left[\left[T(n)-T(n-1)\right]\times\frac{\gamma(n)+\gamma(n-1)}{2}\right] \quad (3)$$

where, $\varepsilon_{thermal}$ (n): thermal deformation,
T(n): the temperature
γ(n): TEC at time n.

By subtracting the thermal deformation from measured total deformation, autogenous shrinkage is calculated.

Fig.8. shows the histories of measured total deformation, thermal deformation and autogenous shrinkage. Autogenous shrinkage at 91 days of $100^2\times400$ and $150^2\times600$ are -324×10^{-6} and -358×10^{-6}. Autogenous shrinkage at 91 days of $300^2\times300$ increases by about 4.8 times (-1550×10^{-6}) compared with that of $100^2\times400$. These results indicate that, although the specimens have the same mixture proportion, as the inner temperature increase, autogenous shrinkage increases. Some reasons for the difference of autogenous shrinkage with inner temperature could be found in the studies of Lothenbach *et al*. (2007, 2008). It was reported that the higher curing temperature lead the following changes; precipitation of a denser inner C-S-H, decrease of the ettringite content at 40°C and above, and differences in morphology of the precipitating ettringite (very short needles at 40°C). These phenomena could lead to an increase in shrinkage. Autogenous shrinkage at 91 days of $300^2\times300$-R decreases by about 6% compared with that of $300^2\times300$.

Table 7. shows the analysis results of ASS, and Fig.9. represents the autogenous shrinkage rise of ASS and shrinkage ratio to autogenous shrinkage at 91 days. Shrinkage ratios of the low hydration temperature specimens ($100^2\times400$ and $150^2\times600$) are lower than the high temperature specimens ($300^2\times300$ and $300^2\times300$-R). ASVs of $100^2\times400$ and $150^2\times600$ are -9.4×10^{-6}/hr. and -9.5×10^{-6}/hr. The ASV of $300^2\times300$ is about 28 times (-267×10^{-6}/hr.) higher than that of 100^2

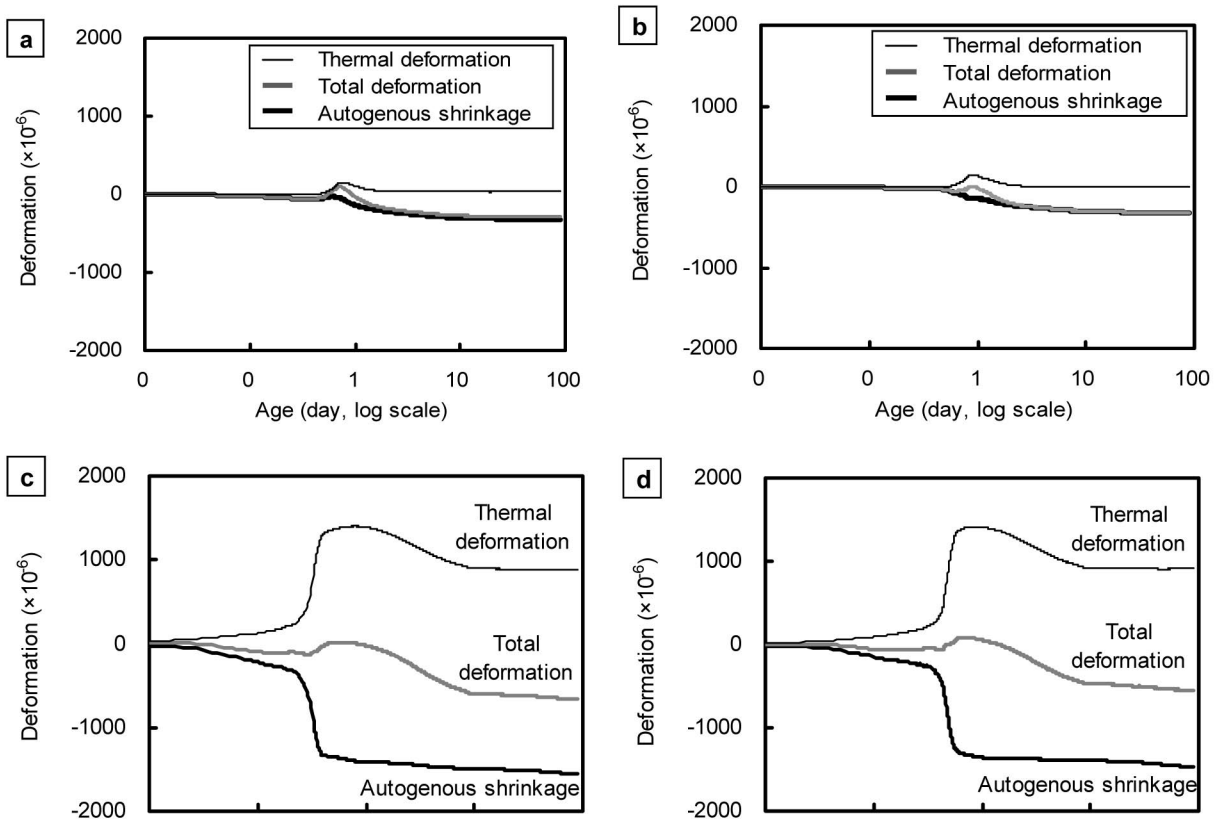

Fig.8. Histories of Measured Total Deformation, Thermal Deformation and Autogenous Shrinkage; (a) $100^2\times400$, (b) $150^2\times600$, (c) $300^2\times300$ and (d) $300^2\times300$-R

Table 7. Analysis Results of ASS

Symbol	Autogenous Shrinking section (ASS)							
	Initial point		Final point		Regression equation	ASV ($\times10^{-6}$/hr.)	Length of time (hr.)	Shrinkage at 91 days ($\times10^{-6}$)
	Time (hr.)	Shrinkage ($\times10^{-6}$)	Time (hr.)	Shrinkage ($\times10^{-6}$)				
$100^2\times400$	16.7	-17	31.8	-166	Y = 117 - 9.40X	-9.4	15.2	-324
$150^2\times600$	10.5	-25	23.2	-136	Y = 70.3 - 9.54X	-9.5	12.7	-358
$300^2\times300$	5.2	-332	8.8	-1243	Y = 1169 - 267X	-267.0	3.7	-1550
$300^2\times300$-R	8.5	-296	12.8	-1166	Y = 1683 - 218X	-218.0	4.3	-1461

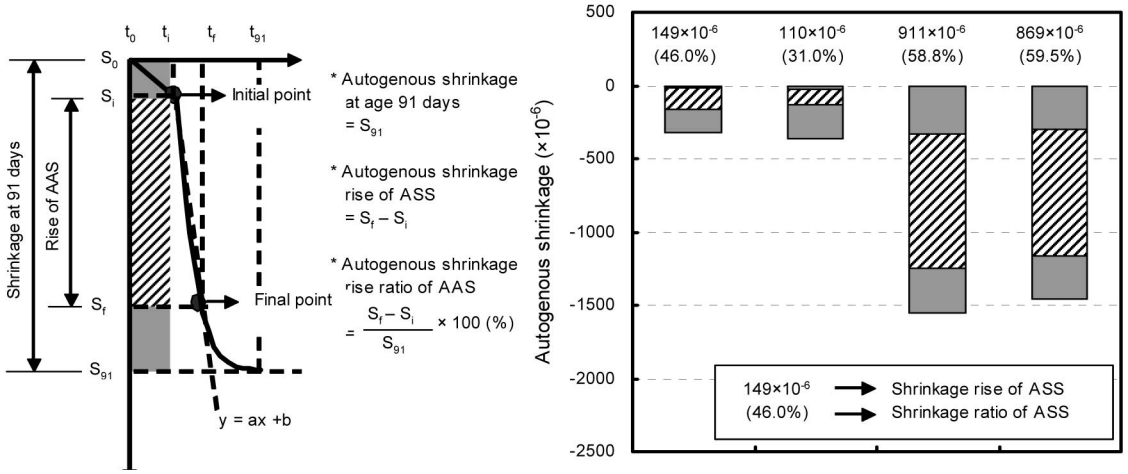

Fig.9. Autogenous Shrinkage Rise of ASS and Shrinkage Ratio to Autogenous Shrinkage at 91 Days

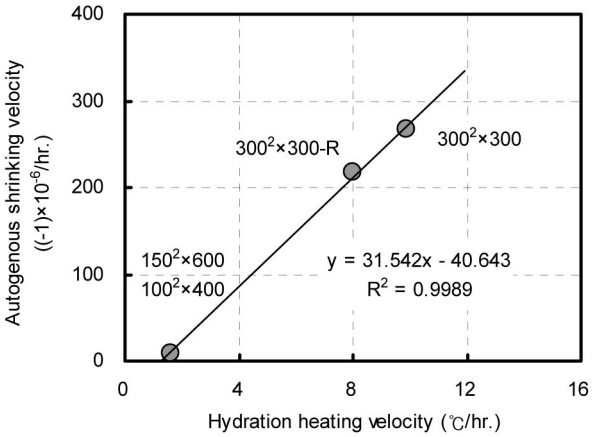

Fig.10. Relation between ASV and Autogenous Shrinkage at 91 Days

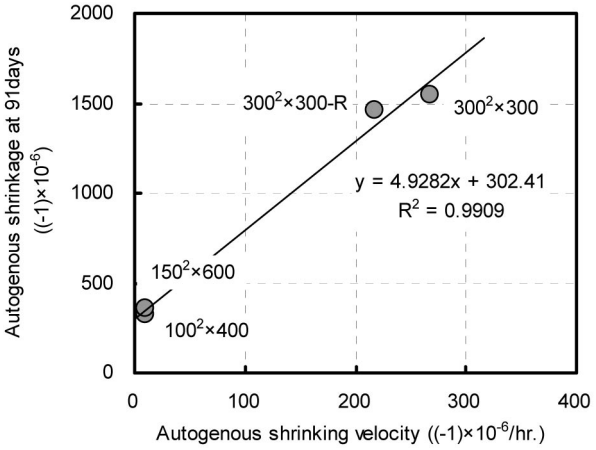

Fig.11. Relation between HHV and ASV

×400. And the ASV of 300^2×300-R is about 80% (-218 $\times 10^{-6}$/hr.) of the 300^2×300's.

3.4 Relation between hydration temperature and autogenous shrinkage

Fig.10. shows the relation between ASV and autogenous shrinkage at 91 days. Autogenous shrinkage at 91 days increases as ASV increases. It could be found that the higher ASV at early ages leads the higher ultimate autogenous shrinkage. The relation between HHV and ASV is presented in Fig.11. It shows the same manner; the higher HHV, the higher ASV. Analyzing synthetically the results of Fig.10. and Fig.11., as HHV increases, ASV and ultimate autogenous shrinkage increase. Also it may be concluded that the ultimate autogenous shrinkage of concrete is affected by HHV at early ages.

3.5 Investigation of the history shape of hydration temperature and autogenous shrinkage

Fig.12. shows the measurement results of hydration temperature, autogenous shrinkage and setting time of the 150×150×600mm mortar specimen. The point where hydration temperature starts to increase, and the bend point are located between the initial setting and the final setting. To investigate changes of cement

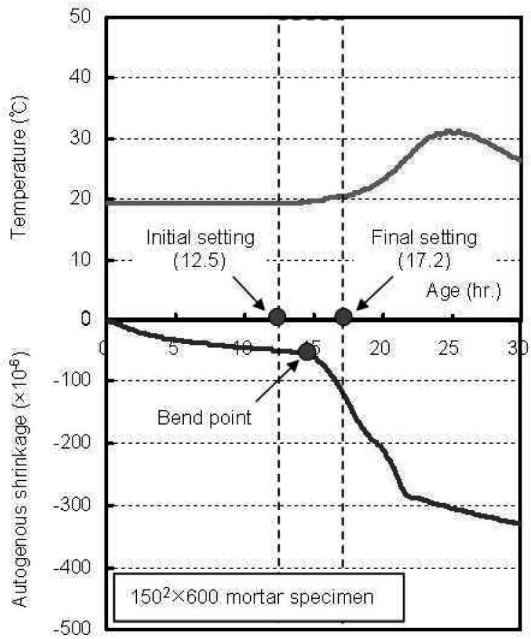

Fig.12. Hydration Temperature, Autogenous Shrinkage and Setting Time of 150×150×600mm Mortar Specimen

compounds and hydrates, four samples were gathered from the cement paste specimen; before the mixing (cement), initial setting time, final setting time and after 1 day. Then XRD analysis on these samples was conducted. The results of the analysis are shown in Fig.13. In cement, the peak of gypsum ($CaSO_4 \cdot H_2O$) is observed. At the initial setting time, the peak of gypsum is decreased and ettringite is observed. At the final setting time, gypsum could not be observed. That said, after mixing of concrete, ettringite is formed by reaction between hydrate and gypsum, and swelling occurs. And, between the initial and final setting, ettringite is transformed to monosulfate and hydration is activated because the gypsum is entirely consumed.

As a result of this phenomenon, the bend point on the history of autogenous shrinkage was observed, and was located in a similar time with the temperature increasing point. The Japan Concrete Institute (1996) noted that the starting time of autogenous shrinkage was the setting time, because the contributions of autogenous shrinkage before setting time to stress development were negligible. That is, the setting time was recognized as a boundary between the liquid and plastic phases in concrete. Therefore, there is a close relationship in the boundary between liquid and plastic phases, setting time, bend point and temperature increasing point from the viewpoint of the chemical reaction of cement.

4. Conclusions

The main conclusions that can be drawn from this study are the following;

1) It is possible to calculate the TEC of high-strength concrete under high temperature by the maturity

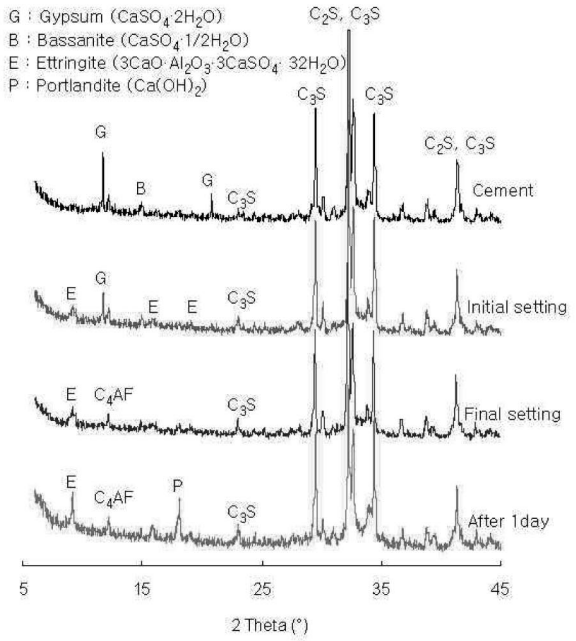

Fig.13. XRD Analysis Results of the Samples Gathered at before the Mixing (Cement), Initial Setting Time, Final Setting Time and after 1 Day

method, and to separate autogenous shrinkage by subtracting the thermal deformation, calculated with the TEC, from total deformation.

2) Hydration temperature is affected by specimen conditions such as size and admixture, and change of hydration temperature could affect autogenous shrinkage; the higher hydration temperature, the greater autogenous shrinkage.

3) There is a close relationship between hydration temperature and autogenous shrinkage at early ages, especially between HHV and ASV; the higher HHV, the higher ASV and the greater ultimate autogenous shrinkage.

4) The points where hydration temperature and autogenous shrinkage start to increase rapidly are due to the consumption of gypsum in the cement hydration process, and are related greatly to the setting time.

Acknowledgement

This work was supported by the Korea Science and Engineering Foundation (KOSEF) grant funded by the Korea Government (MEST) (R01-2007-000-11142-0, 2009-0052476), and some researchers were supported by Brain Korea 2nd (BK21) funded by the Korean Government.

References

1) Aïtcin, P. C. (1999) Autogenous Shrinkage Measurement, Autogenous Shrinkage of Concrete, Ed. E. Tazawa, E&FN Spon, pp.257-268.
2) Bjøntegaard, Ø., Sellevold, E.J. and Hammer, T.A. (1997) High Performance Concrete at Early Ages: Selfgenerated Stresses Due to Autogenous Shrinkage and Temperature, In the Int. Semina : Self-desiccation and its Importance in Concrete Technology, Lund, Sweden, pp.1-7.
3) Horita, T. and Nawa, T. (2001) A Study on Autogenous Shrinkage of Cement Mixes, J. Struct. Constr. Eng., AIJ 542, pp.9-15.
4) Japan Concrete Institute Technical Committee Report on Autogenous Shrinkage (1996) Autogenous Shrinkage of Concrete. Japan Concrete Institute.
5) Kim, G.Y., Lee, E.B, Goo, K.M. and Choi, H.G. (2008) A Fundamental Study on the Correlationship between Hydration Heat and Autogenous Shrinkage of High Strength Concrete at an Early Age, Journal of the Korea Concrete Institute 20(5), pp.593-600.
6) Lee, E.B, Goo, K.M., Kim, G.Y., Lee, S.S., Song, H.Y. (2008) A Study on the Relationship between Hydration Heat and Autogenous Shrinkage of High Strength Concrete, The 7th International Symposium on Architectural Interchanges in Asia, pp.846-849.
7) Lothenbach, B., Winnefeld, F., Alder, C., Wieland, E. and Lunk, P. (2007) Effect of temperature on the pore solution, microstructure and hydration products of Portland cement pastes, Cement and Concrete Research 37, pp.483-491.
8) Lothenbach, B., Matschei, T., Möschner, G. and Glasser, F.P. (2008) Thermodynamic modeling of the effect of temperature on the hydration and porosity of Portland cement, Cement and Concrete Research 38, pp.1-18.
9) Loukili, A., Chopin, D., Khelidj, A. and Touzo, J. L. (2000) A new approach to determine autogenous shrinkage of mortar at an early age considering temperature history, Cement and Concrete Research 30, pp.915-922.
10) Lura, P., Jensen, O. M. and Breugel, K. V. (2003) Autogenous shrinkage in high-performance cement paste: An evaluation of basic mechanism, Cement and Concrete Research 33, pp.223-232.
11) Paillere, A.M., Buil, M. and Serrano, J.J. (1989) Effect of fiber addition on the autogenous shrinkage of silica fume concrete, ACI Material Journal 86 (2), pp.139-144.
12) Turcry, P., Loukili, A., Barcelo, L. and Casabone, J.M. (2002) Can the maturity concept be used to separate the autogenous shrinkage and thermal deformation of a cement paste at early age?, Cement and Concrete Research 32, pp.1443-1450.
13) Shima,T., Matsuda, T., Koide,T., Kawakami, H., Suzuki, Y. and Nishimoto, Y. (2006) Autogenous Shrinkage Characteristic of Ultra High-Strength Concrete Cured under High Temperature (Part1. Experimental Result and Shrinkage Decrease Effect by Expansive Admixture), Proceeding of the architechtural research meetings of AIJ, pp.69-70.
14) Teramoto, A. and Maruyama, I. (2008) Temperature depencency of autogenous shrinkage of silica fume concrete with low W/B ratio, Journal of Structure and Construction Engineering of AIJ 73(634), pp.2069-2076.
15) Yang, Y., Sato, R. and Kawai, K. (2005) Autogenous shrinkage of high-strength concrete containing silica fume under drying at early ages, Cement and Concrete Research 35, pp.449-456.